# Control of the Bright-Dark Exciton Splitting Using the Lamb Shift in a Two-Dimensional Semiconductor

L. Ren (任磊),[1] C. Robert,[1] M. Glazov,[2,*] M. Semina,[2] T. Amand,[1] L. Lombez,[1] D. Lagarde,[1] T. Taniguchi,[3] K. Watanabe,[4] and X. Marie[1,†]

[1]*Université de Toulouse, INSA-CNRS-UPS, LPCNO, 135 Av. Rangueil, 31077 Toulouse, France*
[2]*Ioffe Institute, 26 Polytechnicheskaya, 194021 Saint Petersburg, Russia*
[3]*International Center for Materials Nanoarchitectonics, National Institute for Materials Science, 1-1 Namiki, Tsukuba 305-00044, Japan*
[4]*Research Center for Functional Materials, National Institute for Materials Science, 1-1 Namiki, Tsukuba 305-00044, Japan*

(Received 18 January 2023; accepted 19 July 2023; published 11 September 2023)

We investigate the exciton fine structure in atomically thin $WSe_2$-based van der Waals heterostructures where the density of optical modes at the location of the semiconductor monolayer can be tuned. The energy splitting $\Delta$ between the bright and dark exciton is measured by photoluminescence spectroscopy. We demonstrate that $\Delta$ can be tuned by a few meV as a result of a significant Lamb shift of the optically active exciton that arises from emission and absorption of virtual photons triggered by the vacuum fluctuations of the electromagnetic field. We also measure strong variations of the bright exciton radiative linewidth as a result of the Purcell effect. All these experimental results illustrate the strong sensitivity of the excitons to local vacuum field fluctuations. We find a very good agreement with a model that demonstrates the equivalence, for our system, of a classical electrodynamical transfer matrix formalism and quantum-electrodynamical approach. The bright-dark splitting control we demonstrate here in the weak light-matter coupling regime should apply to any semiconductor structures.

DOI: 10.1103/PhysRevLett.131.116901

Excitons (Coulomb bound electron-hole pairs) play a crucial role for the light-matter coupling in many semiconductor nanostructures [1]. The short range part of the electron-hole exchange interaction yields a splitting of the exciton states corresponding to different relative orientations of electron and hole spins [2–5]. As a result, the lowest energy exciton state is usually a dark, optically inactive, state. In (In)GaAs quantum wells or quantum dots this splitting between bright and dark exciton states is rather small, of the order of hundreds of μeV [6–9]. In 2D perovskites or 2D materials based on transition metal dichalcogenides (TMDs), the dark exciton states can lie tens of meV below the bright ones as a result of larger exchange interaction due to tightly bound excitons and specificities of the band structure [10–17]. In that case the exciton fine structure has a dramatic impact on the emission yield of these new semiconductor nanostructures, even at room temperature [12,13].

So far it has been commonly assumed that the splitting between bright and dark exciton in semiconductors is solely governed by the band structure and the amplitude of the exchange interaction between the electron and the hole. In this Letter we demonstrate that the coupling to light also has to be taken into account [18,19]. We show in our structure a clear tuning of the bright-dark exciton splitting as a result of a significant Lamb shift of the optically active exciton. This shift results from the emission and reabsorption of virtual photons, similarly to atomic systems [20–22]. In contrast, the dark exciton has an oscillator strength orders of magnitude smaller than the bright exciton one yielding a negligible energy shift due to the optical environment. As a consequence, the energy difference between the bright and the dark exciton varies with the characteristics of the electromagnetic field at the location of the semiconductor nanostructure. This can be achieved in a van der Waals heterostructure in the weak light-matter coupling regime as we demonstrate in this Letter.

We have measured the variation of the bright-dark exciton splitting in a 2D semiconductor based on a $WSe_2$ monolayer (ML) encapsulated in hexagonal boron nitride (hBN). The control of the electromagnetic field distribution at the ML plane is simply achieved by changing the thickness of the hBN encapsulation layer; see Fig. 1(a). In a simplified picture, this is equivalent to a variation of the distance between the 2D layer and a mirror whose effective reflectivity is given by the stacking of different layers. The key advantage of this technique is linked to the role of the hBN encapsulation layer that yields narrow optical transitions approaching the homogenous exciton linewidth governed by radiative recombination [23–29]. We measured a variation of the bright-dark

 

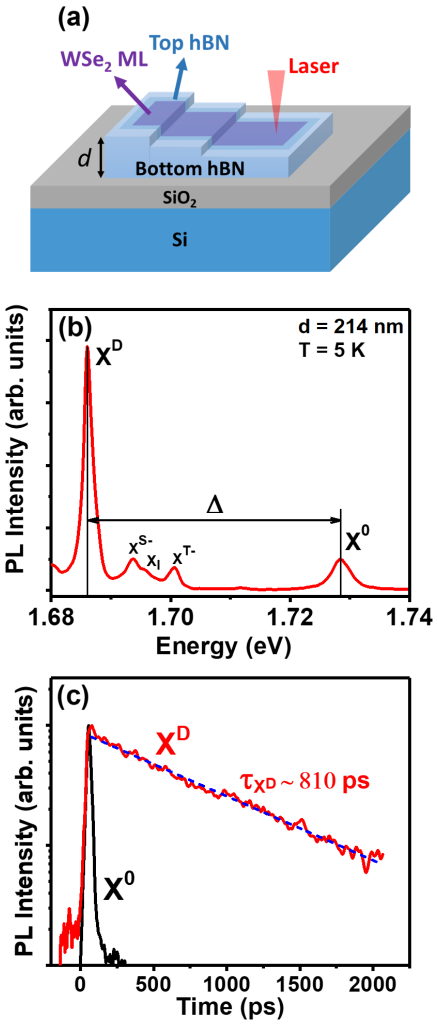


FIG. 1. (a) Schematics of the investigated hBN-encapsulated $WSe_2$ monolayer. (b) CW photoluminescence spectrum of the $WSe_2$ monolayer ($d = 214$ nm) showing mainly the emission of the neutral bright ($X^0$) and dark exciton ($X^D$) at $T = 5$ K; see text. The energy difference between $X^0$ and $X^D$ is denoted $\Delta$. (c) Normalized photoluminescence intensity as a function of time for the neutral bright ($X^0$, black solid line) and dark exciton ($X^D$, red solid line), $d = 290$ nm. The blue dashed line corresponds to a monoexponential fit of the decay time $\tau_{X^D}$.

exciton splitting with the hBN thickness as large as 1.7 meV. This is a consequence of Lamb shifts that are orders of magnitude larger than the ones in atoms owing to the huge exciton oscillator strength in 2D semiconductors [30,31]. The key role of quantum electrodynamics (QED) in these structures is also highlighted by the simultaneous measurement of strong variations of the radiative linewidth, as a result of the Purcell effect [32]. Our measurements are in very good agreement with the calculated dependence of both the radiative linewidth and the bright-dark energy splitting using both transfer matrix techniques and QED approaches. We also uncover a relation between the Purcell and Lamb effects in TMD-based van der Waals heterostructures. We emphasize that the control of the bright-dark exciton splitting demonstrated here for a TMD ML is a general effect obtained in the weak exciton-photon coupling regime and should apply in principle to any semiconductor nanostructures [6,8,9,11].

The investigated samples are $WSe_2$ MLs encapsulated in hBN and deposited onto a $SiO_2/Si$ substrate using a dry-stamping technique; the thickness of the $SiO_2$ layer is 83 nm [33]. Details on the samples and experimental setups can be found in the Supplemental Material (SM) [34].

A $WSe_2$ ML is deposited on a hBN flake exhibiting different terraces and steps with hBN thicknesses $d$ measured during the sample fabrication by atomic force microscopy, Fig. 1(a).

Figure 1(b) displays the photoluminescence (PL) spectrum for $d = 214$ nm at $T = 5$ K using a He-Ne laser (633 nm). In agreement with previous reports, the luminescence of the $WSe_2$ ML is dominated by the recombination of the neutral bright exciton ($X^0$) and the spin-forbidden dark exciton ($X^D$) with an energy splitting of $\Delta \approx 41$ meV [12–17]. The optical selection rules dictate that the $X^D$ exciton is optically forbidden for in-plane polarized light but it can couple to $z$-polarized light [51]. Here, the light propagates mainly along $z$ (perpendicular to the ML plane) but we use a microscope objective with high numerical aperture (NA = 0.82), yielding the detection of a fraction of $z$-polarized luminescence [15,51]. As the dark exciton $X^D$ lies at lower energy compared to the bright exciton, its significant population yields the rather strong PL intensity observed in Fig. 1(b). We also observe much weaker PL components, associated to the recombination of singlet ($X^{S-}$) and triplet ($X^{T-}$) negatively charged excitons and indirect exciton $X_I$ as already identified in many reports [52–54].

Figure 1(c) presents the time evolution of both bright ($X^0$) and dark ($X^D$) exciton luminescence following a picosecond excitation laser pulse in a $WSe_2$ monolayer with $d = 290$ nm. As already measured previously, the $X^0$ lifetime is very short, typically less than 2 ps as a result of the fast radiative recombination time of excitons in TMDs [26,55]. In contrast, we measure a much longer PL decay time, ~800 ps, for the dark exciton $X^D$. This result tells us that the dark exciton oscillator strength is at least 3 orders of magnitude weaker than the bright exciton one, in agreement with theoretical estimates [51]. As a consequence, we can assume that the Lamb shift of the dark exciton is negligible compared to the possible energy shift of the bright exciton linked to absorption or emission of virtual photons. Moreover, since the dark exciton modes are $z$-polarized, they do not experience any cavitylike effect in our structure.

First, we investigate the dependence of the $X^0$ luminescence linewidth as a function of $d$. Figure 2(a) displays the normalized PL spectra for $d = 101$ and 186 nm. We

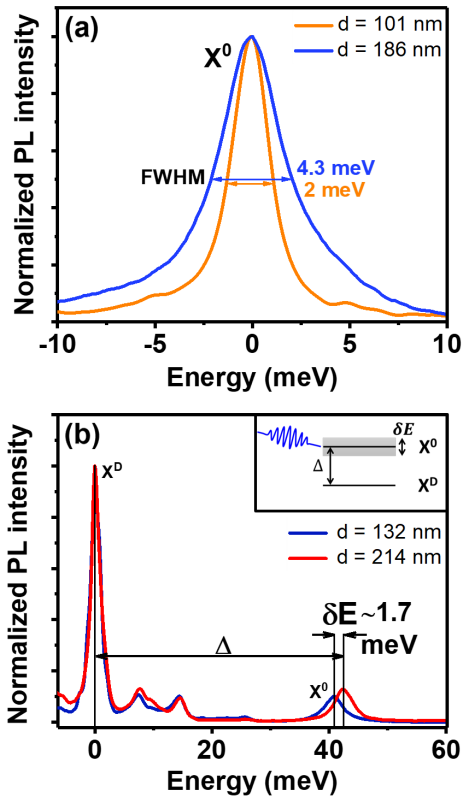


FIG. 2. (a) Normalized CW PL intensity of the neutral exciton for $d = 101$ nm and $d = 186$ nm. In order to compare the linewidths, the origin of the energy axis is taken at the PL peak. The double arrow lines indicate the FWHM linewidths. (b) Normalized PL spectra for $d = 132$ nm and $d = 214$ nm. The energy axis is taken at the $X^D$ PL peak. Inset: schematics of the transition energy shift of $X^0$ (gray shadow) due to Lamb shift.

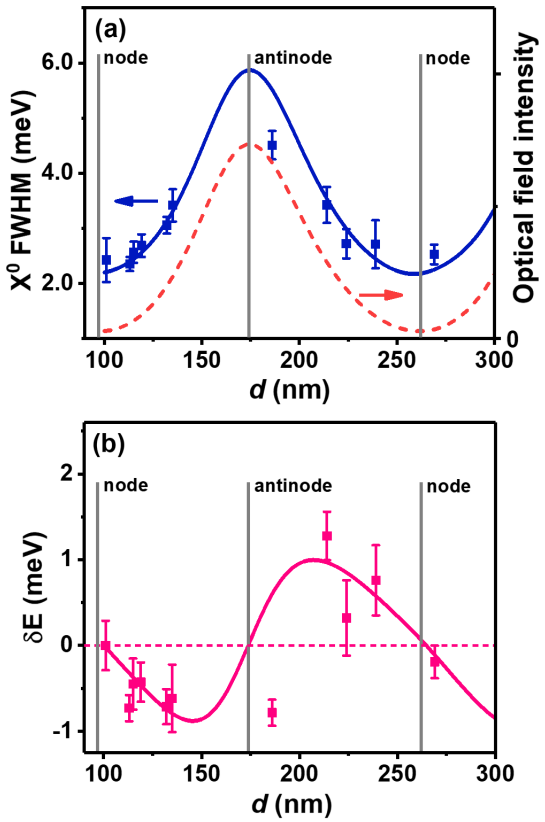


FIG. 3. (a) Measured (blue symbols) and calculated (blue solid line) neutral bright exciton linewidth as function of the bottom hBN thickness $d$. The red dashed curve is the calculated optical field intensity at the monolayer plane. The thickness where the ML is located at the nodes and antinodes are indicated by the vertical gray bars. (b) Measured (pink symbols) and calculated (pink solid line) variation $\delta E$ of the bright-dark exciton splitting as a function of $d$.

observe a clear increase by more than a factor of 2 (4.3 meV compared to 2 meV) in the luminescence full width half maximum (FWHM). As shown in Fig. 3(a), $d = 101$ nm and $d = 186$ nm correspond to position of the ML at the node and the antinode of the optical field intensity respectively in the cavitylike structure (calculations based on the transfer matrix method [56]). Thus the larger PL linewidth in Fig. 2(a) for $d = 186$ nm reflects the decrease of the radiative recombination time due to Purcell effect already observed in $MoSe_2$ MLs [26–28,57]. Figure 3(a) presents the variation of $X^0$ FWHM for 11 values of $d$, confirming the clear control of the linewidth due to the cavitylike effect (see also differential reflectivity measurements in SM [34]). In order to reduce uncertainties, each value displayed in Fig. 3(a) is the average of about 20 measurements obtained at different points of the ML flake for a fixed $d$. The novelty here is the demonstration of the effect in $WSe_2$ monolayer. In contrast to $MoSe_2$, the bright exciton in $WSe_2$ monolayer lies *above* the dark exciton $X^D$, as shown in Fig. 1(b). The clear dependence of the bright exciton linewidth evidenced in Fig. 2(a) demonstrates that it is dominated by the radiative recombination and that the relaxation channel from cold bright exciton to the lower lying dark exciton plays a minor role.

Figures 2(b) and 3(b) present the key result of this Letter. We have measured the bright-dark exciton splitting $\Delta$ for the same samples and hBN thicknesses $d$ as the ones used for the investigation of the Purcell effect. Figure 2(b) displays for instance the PL spectra for $d = 132$ and $d = 214$ nm (the energy origin has been chosen at the dark exciton $X^D$ energy). We observe very clearly a variation $\delta E \approx 1.7$ meV of the splitting. The variation $\delta E$ of the bright-dark splitting as a function of $d$ is displayed in Fig. 3(b). Note that the splitting between $X^0$ and $X^D$ is $\Delta + \delta E$, choosing $\delta E = 0$ for $d = 100$ nm, i.e., when the $WSe_2$ ML is at the node of the electric field in the cavitylike structure. We evidence a significant and oscillatory modulation of $\delta E$ as a function of the electromagnetic field amplitude. These results demonstrate that the energy difference between bright and dark excitons is not only controlled by electron-hole Coulomb exchange interaction and the semiconductor band structure parameters but the

coupling to the electromagnetic field also has to be considered.

Both the exciton linewidth variation and the tuning of the bright-dark exciton energy splitting presented in Fig. 3 can be well understood on the basis of a model based on transfer matrix formalism and quantum-electrodynamical approaches (see Supplemental Material [34]). We have calculated the linear response functions (reflectivity, transmission, and absorbance) of our stacking "top hBN layer/$WSe_2$ ML/bottom hBN layer/$SiO_2$/Si" with the measured 10 nm top hBN thickness, 83 nm $SiO_2$ thickness, and crucially the variable bottom hBN thickness $d$. We used the following refractive indices: $n_{\mathrm{hBN}} = 2.2$, $n_{\mathrm{SiO2}} = 1.46$, $n_{\mathrm{Si}} = 3.5$ [56].

The full line in Fig. 3(a) is the calculated dependence of the bright exciton linewidth $\Gamma = \Gamma_0 + \Gamma_{\mathrm{nr}}$, where $\Gamma_0$ and $\Gamma_{\mathrm{nr}}$ are the radiative and nonradiative contributions, respectively, extracted from the calculated absorption spectrum. We observe a very good agreement between the measured and calculated dependence using the exciton radiative rate in vacuum $\Gamma_0^{\mathrm{vac}} = 2$ meV and $\Gamma_{\mathrm{nr}} = 0.6$ meV. Note that the radiative decay rate is consistent with previous experimental and theoretical estimations of the recombination rate in $WSe_2$ monolayer where the cavity effect was not considered [55,58,59]. Remarkably the same parameters in the model also yield a very good description of the dependence of the exciton bright-dark splitting as a consequence of the Lamb shift; see the full line in Fig. 3(b). The discrepancy observed for $d = 186$ nm could be due to an anomalously large value of the residual doping density for this point attested by a very large trion PL intensity; see SM [34] for details.

In quantum electrodynamics, both the variation of the radiative decay rate and energy of the exciton stem from its coupling with vacuum fluctuations of electromagnetic field. Change in the bottom hBN thickness $d$ changes the local structure of electromagnetic modes in the system and, consequently, $\Gamma_0$ and $\delta E$. The analysis in SM [34] shows that these quantities can be also evaluated semiclassically using the transfer matrix method and expressed via the electrodynamical Green's function. Compact analytical expressions can be derived neglecting the cap layer effect. In that case [26,34],

$$\Gamma_0 + \mathrm{i}\delta E = \Gamma_0^{\mathrm{vac}}(1 + r_{bg}), \tag{1}$$

where $r_{bg}$ is the complex reflection coefficient of a three-layer structure "hBN/$SiO_2$/Si." Thus, the Purcell factor and Lamb shift are proportional to the real and imaginary parts of the substrate's reflection coefficient. It is instructive to consider an illustrative case of a simplified open cavity structure based on a $WSe_2$ ML lying at a distance $d'$ from a nonabsorbing mirror characterized by a real reflection coefficient $r$ (inset in Fig. 4) [31]. In that case $r_{bg} = r\exp(2\mathrm{i}qd')$, $q = \omega/c$, $c$ is the speed of light and

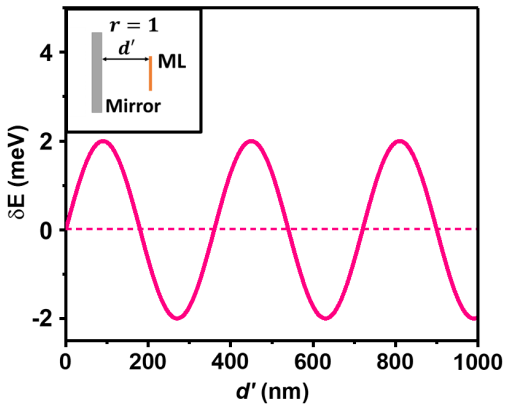


FIG. 4. Calculated variation $\delta E$ of the bright-dark exciton splitting as a function of the distance $d'$ between the mirror (with reflection coefficient $r = 1$) and the WSe2 monolayer. Inset: schematics of the simple configuration where the monolayer is at a distance d' from the mirror.

$\hbar\omega$ the exciton energy; the exciton radiative linewidth and the bright-dark splitting variation write simply [34]

$$\Gamma_0 = \Gamma_0^{\mathrm{vac}}[1 + r\cos(2qd')], \tag{2a}$$

$$\delta E = r\Gamma_0^{\mathrm{vac}}\sin(2qd'). \tag{2b}$$

These simple expressions directly show why the two measurements are in quadrature in Fig. 3. In contrast to the linewidth, which exhibits as expected minima and maxima at the nodes and antinodes, respectively, the bright-dark splitting variation $\delta E$ is strictly zero for these two positions, in perfect agreement with Eq. (2b). Such a behavior is general and follows from the dispersion relations for the reflectivity in Eq. (1); see SM [34] for details. Figure 4 presents the calculated dependence of the bright-dark splitting energy variation for a $WSe_2$ monolayer in this simple "open cavity" composed of a mirror with a 100% reflection coefficient; we used here the same exciton radiative rate in vacuum $\Gamma_0^{\mathrm{vac}} = 2$ meV as the one used in the calculated curves in Fig. 3. A variation of the bright-dark splitting as large as 4 meV due to the Lamb shift can be obtained. These huge variations result from Lamb shift orders of magnitude larger than the ones evidence in atomic systems [18–22,60].

It was recognized so far that the bright-dark exciton splitting $\Delta$ in TMD semiconductor monolayers includes three contributions [16,59]: $\Delta_3 = \Delta_{\mathrm{exch}} + \Delta_{\mathrm{SO}} + \Delta_{\mathrm{bind}}$, where $\Delta_{\mathrm{exch}}$ is the short range exciton exchange energy, $\Delta_{\mathrm{SO}}$ is the conduction band spin-orbit splitting, $\Delta_{\mathrm{bind}}$ is the difference between the binding energies of bright and dark excitons. The terms $\Delta_{\mathrm{SO}}$ and $\Delta_{\mathrm{bind}}$ are due to the specific band structure of TMD monolayers, whereas the exchange term is $\Delta_{\mathrm{exch}} \sim 10$ meV [54,61,62]. In Fig. 4, we show that the new contribution due to QED effect, $\delta E$, could be as large as 4 meV, i.e., ~40% of the exchange term resulting in

$\Delta = \Delta_3 + \delta E$. We can anticipate that similar effects should occur in other TMD monolayers, including $WS_2$ and $MoS_2$ [62–65]. For $MoSe_2$ monolayers, the impact of the optical environment could be even more striking since the dark exciton lies slightly above the bright one with reported values of $\Delta = -1.5$ meV [17,66], i.e., of the order of the energy shifts we have observed in $WSe_2$ MLs, Fig. 3(b). This means that a proper engineering of the vacuum field quantum fluctuations should reverse the bright-dark exciton ordering in $MoSe_2$ MLs. We emphasize that this should occur in *the weak coupling regime*, in contrast to the change of bright-dark ordering evidenced for exciton-polaritons *in the strong coupling regime* for a $WSe_2$ monolayer placed inside a high finesse optical cavity [67]. In GaAs quantum wells, the free exciton oscillator strength is typically ∼10 times weaker than the one in TMD monolayers [68]; thus Eq. (2b) predicts a typical variation of the bright-dark splitting of the order of ∼100 μeV (using $r = 1$). Remarkably this value is similar to the bright-dark splitting due to the exchange interaction measured in GaAs/AlGaAs quantum wells [6,7]. For 2D perovskites significant variations of the exciton bright-dark splitting are also expected [10].

Finally we can note that the electromagnetic quantum fluctuations could also impact long-range exchange interaction in the exciton, as theoretically predicted both in bulk and 2D semiconductors [1,69,70].

In conclusion we have shown that not only the exciton radiative lifetime is controlled by the optical environment in a 2D semiconductor but the bright-dark exciton splitting can also be modified by the potential induced by quantum fluctuations of the electromagnetic field. All these results show that the excitons in semiconductor nanostructures are very sensitive probes of the local vacuum field.

This work was supported by the French Agence Nationale de la Recherche under the program ESR/EquipEx+ (Grant No. ANR-21-ESRE-0025) and the ANR projects ATOEMS, Sizmo-2D and Magicvalley.

L. R., C. R., and M. G. contributed equally to this work.

*Corresponding author: glazov@coherent.ioffe.ru
†Corresponding author: marie@insa-toulouse.fr

[1] E. L. Ivchenko, *Optical Spectroscopy of Semiconductor Nanostructures* (Alpha Science, Harrow, 2005).
[2] G. E. Pikus and G. L. Bir, Exchange interaction in excitons in semiconductors, Sov. Phys. JETP **33**, 108 (1971), http://www.jetp.ras.ru/cgi-bin/dn/e_033_01_0108.pdf.
[3] M. M. Denisov and V. P. Makarov, Longitudinal and transverse excitons in semiconductors, Phys. Status Solidi (b) **56**, 9 (1973).
[4] L. C. Andreani and F. Bassani, Exchange interaction and polariton effects in quantum-well excitons, Phys. Rev. B **41**, 7536 (1990).
[5] M. Combescot and M. N. Leuenberger, General argument supporting Bose–Einstein condensate of dark excitons in single and double quantum wells, Solid State Commun. **149**, 567 (2009).
[6] E. Blackwood, M. J. Snelling, R. T. Harley, S. R. Andrews, and C. T. B. Foxon, Exchange interaction of excitons in GaAs heterostructures, Phys. Rev. B **50**, 14246 (1994).
[7] T. Amand, X. Marie, P. Le Jeune, M. Brousseau, D. Robart, J. Barrau, and R. Planel, Spin Quantum Beats of 2D Excitons, Phys. Rev. Lett. **78**, 1355 (1997).
[8] M. Bayer *et al.*, Fine structure of neutral and charged excitons in self-assembled In(Ga)As/(Al)GaAs quantum dots, Phys. Rev. B **65**, 195315 (2002).
[9] E. Poem, Y. Kodriano, C. Tradonsky *et al.*, Accessing the dark exciton with light, Nat. Phys. **6**, 993 (2010).
[10] M. Dyksik, H. Duim, D. K. Maude, M. Baranowski, M. A. Loi, and P. Plochocka, Brightening of dark excitons in 2D perovskites, Sci. Adv. **7**, eabk0904 (2021).
[11] M. Gramlich, M. W. Swift, C. Lampe, J. L. Lyons, M. Döblinger, A. L. Efros, P. C. Sercel, and A. S. Urban, Dark and bright excitons in halide perovskite nanoplatelets, Adv. Sci. **9**, 2103013 (2022).
[12] X.-X. Zhang, Y. You, Shu Yang Frank Zhao, and T. F. Heinz, Experimental Evidence for Dark Excitons in Monolayer $WSe_2$, Phys. Rev. Lett. **115**, 257403 (2015).
[13] G. Wang *et al.*, Spin-orbit engineering in transition metal dichalcogenide alloy monolayers, Nat. Commun. **6**, 10110 (2015).
[14] A. Arora, M. Koperski, K. Nogajewski, J. Marcus, C. Faugeras, and M. Potemski, Excitonic resonances in thin films of $WSe_2$: From monolayer to bulk material, Nanoscale **7**, 10421 (2015).
[15] G. Wang *et al.*, In-Plane Propagation of Light in Transition Metal Dichalcogenide Monolayers: Optical Selection Rules, Phys. Rev. Lett. **119**, 047401 (2017).
[16] M. Zinkiewicz *et al.*, Neutral and charged dark excitons in monolayer $WS_2$, Nanoscale **12**, 18153 (2020).
[17] C. Robert *et al.*, Measurement of the spin-forbidden dark excitons in $MoS_2$ and $MoSe_2$ Monolayers, Nat. Commun. **11**, 4037 (2020).
[18] W. E. Lamb and R. C. Retherford, Fine structure of the hydrogen atom by a microwave method, Phys. Rev. **72**, 241 (1947).
[19] H. A. Bethe, The electromagnetic shift of energy levels, Phys. Rev. **72**, 339 (1947).
[20] R. Friedberg, S. R. Hartmann, and J. T. Manassah, Frequency shifts in emission and absorption by resonant systems of two-level atoms, Phys. Rep. **7**, 101 (1973).
[21] R. Röhlsberger, K. Schlage, B. Sahoo, S. Couet, and R. Rüffer, Collective Lamb shift in single-photon superradiance, Science **328**, 1248 (2010).
[22] J. Keaveney, A. Sargsyan, U. Krohn, I. G. Hughes, D. Sarkisyan, and C. S. Adams, Cooperative Lamb Shift in an Atomic Vapor Layer of Nanometer Thickness, Phys. Rev. Lett. **108**, 173601 (2012).
[23] F. Cadiz, E. Courtade, C. Robert, G. Wang, Y. Shen *et al.*, Excitonic Linewidth Approaching the Homogeneous Limit in $MoS_2$-Based van Der Waals Heterostructures, Phys. Rev. X **7**, 021026 (2017).

[24] O. A. Ajayi *et al.*, Approaching the intrinsic photoluminescence linewidth in transition metal dichalcogenide monolayers, 2D Mater. **4**, 031011 (2017).

[25] P. Back, S. Zeytinoglu, A. Ijaz, M. Kroner, and A. Imamoğlu, Realization of an Electrically Tunable Narrow-Bandwidth Atomically Thin Mirror Using Monolayer $MoSe_2$, Phys. Rev. Lett. **120**, 037401 (2018).

[26] H. H. Fang *et al.*, Control of the Exciton Radiative Lifetime in van Der Waals Heterostructures, Phys. Rev. Lett. **123**, 067401 (2019).

[27] Y. Zhou *et al.*, Controlling Excitons in an Atomically Thin Membrane with a Mirror, Phys. Rev. Lett. **124**, 027401 (2020).

[28] C. Rogers, D. Gray, N. Bogdanowicz, T. Taniguchi, K. Watanabe, and H. Mabuchi, Coherent feedback control of two-dimensional excitons, Phys. Rev. Res. **2**, 012029(R) (2020).

[29] E. W. Martin, J. Horng, H. G. Ruth, E. Paik, M.-H. Wentzel, H. Deng, and S. T. Cundiff, Encapsulation Narrows and Preserves the Excitonic Homogeneous Linewidth of Exfoliated Monolayer $MoSe_2$, Phys. Rev. Appl. **14**, 021002(R) (2020).

[30] G. Frucci, S. Huppert, A. Vasanelli, B. Dailly, Y. Todorov, G. Beaudoin, I. Sagnes, and C. Sirtori, Cooperative Lamb shift and superradiance in an optoelectronic device, New J. Phys. **19**, 043006 (2017).

[31] J. Horng, Y.-H. Chou, T.-C. Chang, C.-Y. Hsu, T.-C. Lu, and H. Deng, Engineering radiative coupling of excitons in 2D semiconductors, Optica **6**, 1443 (2019).

[32] E. Purcell, Proceedings of the American Physical Society, Phys. Rev. **69**, 674 (1946).

[33] A. Castellanos-Gomez, M. Buscema, R. Molenaar, V. Singh, L. Janssen, H. S. J. van der Zant, and G. A. Steele, Deterministic transfer of two-dimensional materials by all-dry viscoelastic stamping, 2D Mater. **1**, 011002 (2014).

[34] See Supplemental Material, which includes [35–50], at http://link.aps.org/supplemental/10.1103/PhysRevLett.131.116901 for additional experimental data and theory of spontaneous emission in van der Waals heterostructure.

[35] C. Robert *et al.*, Measurement of Conduction and Valence Bands g Factors in a Transition Metal Dichalcogenide Monolayer, Phys. Rev. Lett. **126**, 067403 (2021).

[36] J. G. Roch, G. Froehlicher, N. Leisgang, P. Makk, K. Watanabe, T. Taniguchi, and R. J. Warburton, Spin-polarized electrons in monolayer $MoS_2$, Nat. Nanotechnol. **14**, 432 (2019).

[37] P. Back, M. Sidler, O. Cotlet, A. Srivastava, N. Takemura, M. Kroner, and A. Imamoğlu, Giant Paramagnetism-Induced Valley Polarization of Electrons in Charge-Tunable Monolayer $MoSe_2$, Phys. Rev. Lett. **118**, 237404 (2017).

[38] J. D. E. McIntyre and D. E. Aspnes, Differential reflection spectroscopy of very thin surface films, Surf. Sci. **24**, 417 (1971).

[39] F. De Martini, M. Marrocco, P. Mataloni, L. Crescentini, and R. Loudon, Spontaneous emission in the optical microscopic cavity, Phys. Rev. A **43**, 2480 (1991).

[40] A. I. Akhiezer and V. B. Berestetskiĭ, *Quantum Electrodynamics* (Interscience Publishers, 1965).

[41] V. B. Berestetskii, E. M. Lifshitz, and L. P. Pitaevskii, *Quantum Electrodynamics*, 2nd ed. (Butterworth-Heinemann, Oxford, 1999), Vol. 4.

[42] M. M. Glazov, T. Amand, X. Marie, D. Lagarde, L. Bouet, and B. Urbaszek, Exciton fine structure and spin decoherence in monolayers of transition metal dichalcogenides, Phys. Rev. B **89**, 201302(R) (2014).

[43] M. M. Glazov, E. L. Ivchenko, A. N. Poddubny, and G. Khitrova, Purcell factor in small metallic cavities, Phys. Solid State **53**, 1753 (2011).

[44] V. Lucarini, F. Bassani, K. E. Peiponen, and J. J. Saarinen, Dispersion theory and sum rules in linear and nonlinear optics, Riv. Nuovo Cimento **26**, 1 (2003).

[45] K.-E. Peiponen, E. Gornov, Y. Svirko, Y. Ino, M. Kuwata-Gonokami, and V. Lucarini, Testing the validity of terahertz reflection spectra by dispersion relations, Phys. Rev. B **72**, 245109 (2005).

[46] B. Gralak, Analytic properties of the electromagnetic Green's function, J. Math. Phys. (N.Y.) **58**, 071501 (2017).

[47] R. A. Suris *et al.*, Excitons and trions modified by interaction with a two-dimensional electron gas, Phys. Status Solidi (b) **227**, 343 (2001).

[48] M. Sidler, P. Back, O. Cotlet, A. Srivastava, T. Fink, M. Kroner, E. Demler, and A. Imamoglu, Fermi polaron-polaritons in charge-tunable atomically thin semiconductors, Nat. Phys. **13**, 255 (2017).

[49] M. M. Glazov, Optical properties of charged excitons in two-dimensional semiconductors, J. Chem. Phys. **153**, 034703 (2020).

[50] Z. A. Iakovlev and M. M. Glazov, Fermi polaron fine structure in strained van der Waals heterostructures, 2D Mater. **10**, 035034 (2023).

[51] J. P. Echeverry, B. Urbaszek, T. Amand, X. Marie, and I. C. Gerber, Splitting between bright and dark excitons in transition metal dichalcogenide monolayers, Phys. Rev. B **93**, 121107(R) (2016).

[52] A. M. Jones, H. Yu, J. R. Schaibley, J. Yan, D. G. Mandrus, T. Taniguchi, K. Watanabe, H. Dery, W. Yao, and X. Xu, Excitonic luminescence upconversion in a two-dimensional semiconductor, Nat. Phys. **12**, 323 (2016).

[53] E. Courtade, M. Semina, M. Manca, M. M. Glazov, C. Robert *et al.*, Charged excitons in monolayer $WSe_2$: Experiment and theory, Phys. Rev. B **96**, 085302 (2017).

[54] M. He *et al.*, Valley phonons and exciton complexes in a monolayer semiconductor, Nat. Commun. **11**, 618 (2020).

[55] C. Robert *et al.*, Exciton radiative lifetime in transition metal dichalcogenide monolayers, Phys. Rev. B **93**, 205423 (2016).

[56] C. Robert *et al.*, Optical spectroscopy of excited exciton states in $MoS_2$ monolayers in van der Waals heterostructures, Phys. Rev. Mater. **2**, 011001(R) (2018).

[57] M. Förg, L. Colombier, R. K. Patel, J. Lindlau, A. D. Mohite, H. Yamaguchi, M. M. Glazov, D. Hunger, and A. Högele, Cavity-control of interlayer excitons in van der Waals heterostructures, Nat. Commun. **10**, 3697 (2019).

[58] M. Palummo, M. Bernardi, and J. C. Grossman, Exciton radiative lifetimes in two-dimensional transition metal dichalcogenides, Nano Lett. **15**, 2794 (2015).

[59] C. Boule, D. Vaclavkova, M. Bartos, K. Nogajewski, L. Zdražil, T. Taniguchi, K. Watanabe, M. Potemski, and J.

Kasprzak, Coherent dynamics and mapping of excitons in single-layer $MoSe_2$ and $WSe_2$ at the homogeneous limit, Phys. Rev. Mater. **4**, 034001 (2020).

[60] Q. Sun, M. Al-Amri, A. Kamli, and M. S. Zubairy, Lamb shift due to surface plasmon polariton modes, Phys. Rev. A **77**, 062501 (2008).

[61] P. Li, C. Robert, D. Van Tuan, L. Ren, M. Yang, X. Marie, and H. Dery, Intervalley electron-hole exchange interaction and impurity-assisted recombination of indirect excitons in $WS_2$ and $WSe_2$ monolayers, Phys. Rev. B **106**, 085414 (2022).

[62] A. Chernikov, T. C. Berkelbach, H. M. Hill, A. Rigosi, Y. Li, O. B. Aslan, D. R. Reichman, M. S. Hybertsen, and T. F. Heinz, Exciton Binding Energy and Nonhydrogenic Rydberg Series in Monolayer $WS_2$, Phys. Rev. Lett. **113**, 076802 (2014).

[63] K. He, N. Kumar, L. Zhao, Z. Wang, K. F. Mak, H. Zhao, and J. Shan, Tightly Bound Excitons in Monolayer $WSe_2$, Phys. Rev. Lett. **113**, 026803 (2014).

[64] G. Wang, X. Marie, I. Gerber, T. Amand, D. Lagarde, L. Bouet, M. Vidal, A. Balocchi, and B. Urbaszek, Giant Enhancement of the Optical Second-Harmonic Emission of $WSe_2$ Monolayers by Laser Excitation at Exciton Resonances, Phys. Rev. Lett. **114**, 097403 (2015).

[65] M. Goryca *et al.*, Revealing exciton masses and dielectric properties of monolayer semiconductors with high magnetic fields, Nat. Commun. **10**, 4172 (2019).

[66] Z. Lu *et al.*, Magnetic field mixing and splitting of bright and dark excitons in monolayer $MoSe_2$, 2D Mater. **7**, 015017 (2019).

[67] H. Shan *et al.*, Brightening of a dark monolayer semiconductor via strong light-matter coupling in a cavity, Nat. Commun. **13**, 3001 (2022).

[68] B. Deveaud, F. Clérot, N. Roy, K. Satzke, B. Sermage, and D. S. Katzer, Enhanced Radiative Recombination of Free Excitons in GaAs Quantum Wells, Phys. Rev. Lett. **67**, 2355 (1991).

[69] A. I. Prazdnichnykh, M. M. Glazov, L. Ren, C. Robert, B. Urbaszek, and X. Marie, Control of the exciton valley dynamics in atomically thin semiconductors by tailoring the environment, Phys. Rev. B **103**, 085302 (2021).

[70] M. Combescot, F. Dubin, and S.-Y. Shiau, Signature of electromagnetic quantum fluctuations in exciton physics, Europhys. Lett. **138**, 36002 (2022).